CHAPTER

6

Tools for Proximal Soil Sensing

By Viacheslav Adamchuk, McGill University; Barry Allred, USDA–ARS; James Doolittle, USDA–NRCS; Katherine Grote, Missouri University of Science and Technology; and Raphael Viscarra Rossel, CSIRO Land and Water

Introduction

Proximal soil sensing is a collection of technologies that employ a sensor close to, or in direct contact with, the soil. The sensor measures a soil property directly or indirectly. Viscarra Rossel et al. (2011) provide a description of proximal soil sensing, sensing technologies, and the soil properties these technologies can measure. This chapter describes different types of proximal sensing tools that can be used to map soil attributes of importance for agriculture and natural resource management.[1]

Soil properties vary in space and over time. As a consequence, they are seldom adequately described at field and landscape scales by traditional soil survey tools. Traditional methods of soil sampling and analyses provide detailed information at specific locations. This information, however, is limited in number, volume, and spatial coverage. See chapter 3 for a discussion of the standards and protocols used to examine and describe soils at the pedon scale in the field. At field and landscape scales, the characterization of the spatial and temporal variations is prohibitively time-consuming, expensive, and impractical using traditional point-sampling methods alone. Remote sensing (e.g., satellite images and aerial photos) can provide excellent spatial coverage, but measurements are mostly indirect and typically limited to the top 5–6 cm of soil. In addition, resolution is generally

[1] Trade or company names used in this chapter are provided as examples for informational purposes only. This use does not constitute an endorsement by USDA or the contributing authors of this chapter.

too coarse to characterize the spatial variability of soil properties at intermediate field and landscape scales. Because of these limitations, proximal soil sensing is becoming increasingly popular as a way to fill in the data gap between high-resolution point data and the lower resolution remote-sensing data (Adamchuk et al., 2011; Adamchuk and Viscarra Rossel, 2011).

Data from proximal soil sensing technologies can be used in soil surveys of order 1, 2, or 3. They can be used to show how one or more soil properties vary over a portion of the landscape, to help estimate the range in property values for a particular soil series or map unit component, to refine the boundaries of soil map unit delineations, and to identify the location and extent of contrasting soil components within soil map unit delineations. Some of the methods can be used to document soil properties at specific locations (point data) when describing soil profiles. Table 6-1 shows the general application of various proximal soil sensing methods to soil survey activities. Definitions of soil survey orders are given in chapter 4.

This chapter is divided into two major parts. The first part discusses three geophysical methods: ground-penetrating radar, electromagnetic induction, and electrical resistivity. These methods have been used widely in the United States by the National Cooperative Soil Survey (NCSS) to document soil property variability in specific landscape settings and to identify the locations of contrasting soil components within map units. The second part discusses nine other proximal soil sensing methods that, to date, have had limited application by the NCSS. These technologies are included in this chapter because they have potential for expanded future use, especially in high-intensity surveys (i.e., order 1) and in recording properties when describing soil profiles.

Common Geophysical Methods

The three geophysical methods most commonly used for soils and agriculture are ground-penetrating radar (GPR), electromagnetic induction (EMI), and electrical resistivity (ER) (Allred et al., 2008a and 2010).

Geophysical methods exploit contrasts in physical properties to indirectly measure, profile, and monitor differences in physico-chemical soil properties; locate soil, lithologic, and stratigraphic boundaries; and characterize soil patterns and features. Examples of the physical

Table 6-1

Methods of Proximal Soil Sensing and Their Primary Application in Soil Survey

[Order 1 surveys are high-intensity or special use surveys. Applications for order 1, 2, and 3 surveys include map unit boundaries, component composition, and/or spatial distribution of properties (see chapter 4). Applications for point data include documentation of static or temporal soil properties.]

Method	Primary soil survey application		
	Map unit (spatial) data		Point data
	Order 1	Orders 2 & 3	
Ground-penetrating radar	X	X	
Electromagnetic induction	X	X	
Electrical resistivity	X	X	
Magnetometry	X		
Magnetic susceptibility	X		
Portable X-ray fluorescence			X
Time domain reflectometry			X
Optical reflectance	X	X	X
Gamma-ray spectroscopy	X	X	X
Mechanical interactions	X		X
Ion-selective potentiometry	X		X
Seismic	X	X	

properties include dielectric permittivity, apparent electrical conductivity or resistivity, and magnetic susceptibility.

ER and EMI methods were initially used to assess soil salinity, but their use greatly expanded with the development of precision agriculture in the 1990s. Since the late 1970s, GPR has been used extensively by the National Cooperative Soil Survey as a quality-control tool to improve soil interpretations. Recent technological improvements have increased the use of these and other geophysical methods in soils. Improvements include instrumentation, computational capabilities, data processing, interpretative and display methods, and integration with other technologies (e.g., global positioning systems).

Ground-Penetrating Radar (GPR)

Ground-penetrating radar is an impulse radar system. It transmits short pulses of very high and ultra-high frequency (from about 30 MHz to 1.2 GHz) electromagnetic energy into the soil and underlying strata from an antenna. When these pulses contact an interface between layers with contrasting dielectric permittivity, a portion of the energy is reflected back to a receiving antenna. The more abrupt and contrasting the difference in dielectric permittivity, the greater the amount of energy that is reflected back to the receiving antenna. The receiving antenna records the amplitude of the reflected energy as a function of time, and the variation in amplitude is displayed on a video screen and stored for playback and processing. Interpretation of GPR data is generally performed by noting the arrival time of a reflection from a subsurface interface and associating the reflection with a known or suspected soil interface. To interpret the depth to an interface, the velocity of the pulse through the soil must be determined or the interface depth must be obtained by ground-truth measurements.

Ground-penetrating radar is most effective at sharp interfaces between materials of contrasting dielectric permittivity. Although influenced by bulk density and mineralogy, dielectric permittivity in soil is primarily controlled by water content. Thus, GPR is useful for imaging the interfaces between layers that contain different amounts of water. It is also very effective in determining the location of air-filled or water-filled voids (such as pipes) and metallic objects. GPR works best in coarse grained soils because electrically conductive materials (i.e., soils with high clay content and saline soils) weaken the signal.

A disadvantage of GPR is that resolution decreases with increasing depth of investigation and decreasing antenna frequency. Although higher frequency antennas provide higher resolution, they also provide lesser depth of investigation. Penetration depth is inversely proportional to the sounding frequency. In general, penetration with low-frequency antennas is less than 30 cm in saline soils and less than 1 m in wet, clayey soils (Daniels, 2004). In dry, sandy and gravelly soils, however, GPR penetration can exceed 50 m with low-frequency antennas (Smith and Jol, 1995). Profiling depths as great as 10 m have been recorded in organic soil materials that have very low electrical conductivity.

The speed, field economy, high resolution, and continuous measurement of GPR are assets in soil investigations. Modern GPR systems are self-contained and portable and have integrated GPS and real-time data visualization capabilities, which allow greater mobility and more effective use (fig. 6-1).

Figure 6-1

Modern GPR systems are light-weight, highly mobile, and integrated. A typical GPR system consists of a control unit (located beneath blue visor on the cart) with an antenna (orange box beneath the cart).

Examples of GPR Use in Soil Survey

Ground-penetrating radar has been used by soil scientists principally in order 1, 2, and 3 soil surveys. It serves as a quality control tool in documenting the taxonomic compositions and improving the interpretations of soil map units (Doolittle and Butnor, 2008). In these applications, GPR documents the presence, depth, lateral extent, and variability of diagnostic subsurface horizons. Typically, strong radar reflections are produced by abrupt interfaces between highly contrasting soil materials. Where soil conditions are suitable, GPR can determine the depth to contrasting master (B, C, and R) subsurface horizons and layers. Other soil horizons and layers have also been identified with GPR. Examples include buried genetic horizons, dense root-restricting layers, frozen soil layers, illuvial accumulations of organic matter, and cemented or indurated horizons. Ground-penetrating radar generally is unable to detect subtle changes in soil properties (e.g., structure, porosity, and texture), transitional horizons (e.g., AB, AC, and BC), or

vertical divisions of master horizons. However, GPR has been used to infer distinct vertical changes in soil color associated with abrupt and contrasting changes in organic carbon content.

Figure 6-2 is a radar record from an area of Pomona soils (sandy, siliceous, hyperthermic Ultic Alaquods) in north-central Florida. The upper boundaries of the spodic and argillic horizons are abrupt and separate contrasting soil materials. They therefore produce high-amplitude reflections. On this radar record, the spodic horizon provides a continuous reflector that varies in depth from about 20 to 60 cm. The upper boundary of the argillic horizon is highly irregular and varies in depth from about 60 to 150 cm. Generally, argillic horizons provide smooth, continuous reflectors at more uniform depths than those shown in this example. The irregular topography of the upper boundary of this argillic horizon is attributed to underlying dissolution features associated with karst. The presence and varying depths to these two subsurface soil horizons were used to distinguish different soils along the radar traverse line.

Figure 6-2

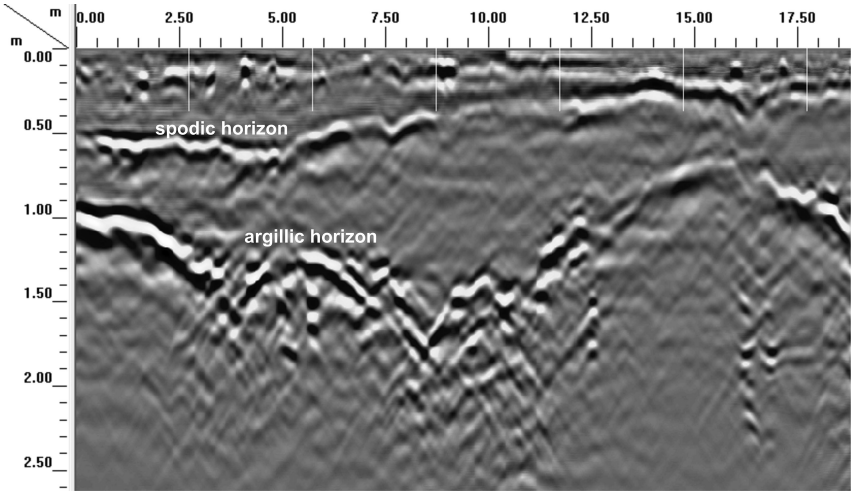

A radar record showing well expressed spodic and argillic horizons in a Pomona soil in north-central Florida.

The radar record in figure 6-3 shows an abrupt and contrasting discontinuity that separates a silty eolian mantle from underlying sandy outwash. This stratigraphic discontinuity is an easily identified, laterally

continuous, high-amplitude reflector that ranges in depth from about 85 to 150 cm across the radar record. In southern Rhode Island, the depth to the discontinuity was used to distinguish areas of Bridgehampton soils (coarse-silty, mixed, active, mesic Typic Dystrudepts) and Enfield soils (coarse-silty over sandy or sandy-skeletal, mixed, active, mesic Typic Dystrudepts). Soil materials on different sides of this discontinuity differ from each other substantially in particle-size distribution, bulk density, and pore-size distribution. In addition, linear reflections in the lower material helped to confirm that the material is glacial outwash rather than till. Typically, till has a chaotic radar signature characterized by an abundance of point reflectors (from cobbles and boulders) and an absence of linear reflectors (which are typical for layered deposits). On this radar record, a dense Bw horizon appears as a weakly expressed linear reflector at a depth of about 35 cm.

Figure 6-3

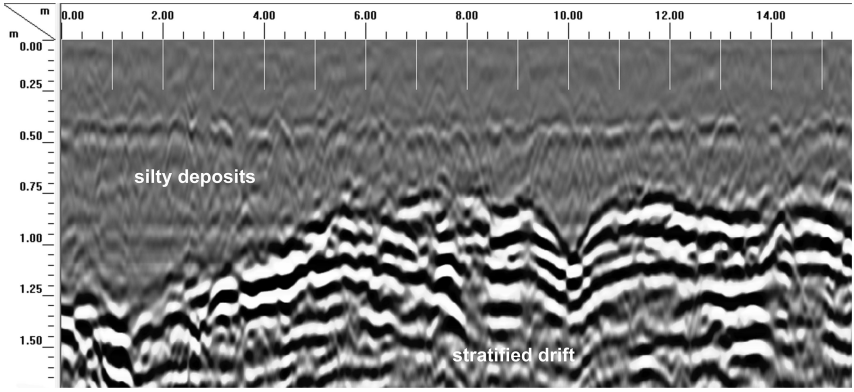

A radar record showing a discontinuity separating a loamy eolian mantle from sandy glacial outwash in southern Rhode Island.

Hydropedological modeling requires detailed information on the depth and movement of water beneath soil landscapes. Sandy soils have a narrow capillary fringe, resulting in a relatively sharp interface between unsaturated and saturated soil materials. As a result, water tables are often distinguishable on radar records from sandy soils.

Figure 6-4 is a surface normalized (i.e., elevation data were used to show topographic changes) radar record. It shows a low dune composed of very deep, excessively drained Oakville soils (mixed, mesic Typic

Udipsamments) in northwestern Indiana. On this radar record, the water table can be seen as a continuous, high-amplitude reflector between depths of about 2.5 and 4.0 m. Repetitive GPR measurements throughout the year can increase the level of confidence in hydropedological site assessments and reduce the number of wells needed for studies of water tables and ground-water flow.

Figure 6-4

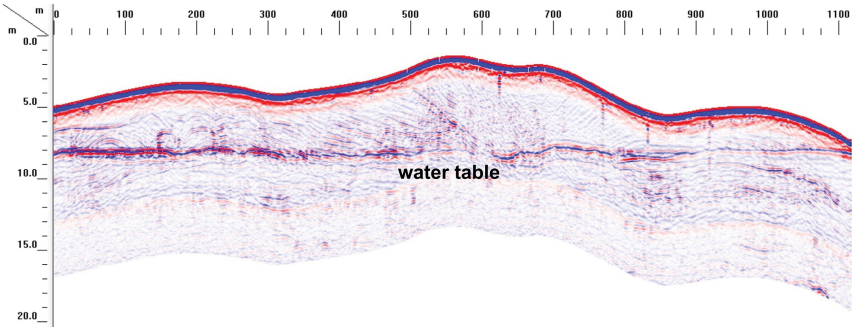

A terrain-corrected radar record in which a water table provides a high-amplitude reflector in a dune field in Indiana.

Ground-penetrating radar has been used extensively on peatlands. GPR applications in peatlands include estimating the thickness and volume of peat deposits; distinguishing layers that differ in degree of humification, bulk density, and volumetric water content; characterizing underlying mineral sediments, stratigraphy, and hydrology and their relationships to present vegetation; and classifying and mapping organic soils.

Figure 6-5 is a radar record from a fen in a kettle depression in southeastern Massachusetts. The fen is an area of very deep, very poorly drained Freetown soils (dysic, mesic Typic Haplosaprists). Abrupt and strongly contrasting changes in water content make the interface between organic and mineral material distinguishable on the radar record. This interface forms a conspicuous reflection that varies in depth from about 0.36 meter to 5.4 meters.

In addition to detecting subsurface interfaces, GPR can be used as a tool for quantitatively mapping soil water content (Huisman et al., 2003). This mapping can be done because of the strong dependence of dielectric permittivity on soil water content. The dielectric permittivities of air and

Figure 6-5

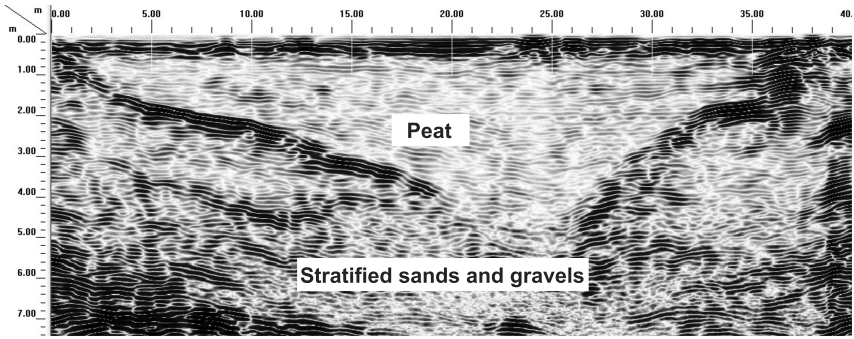

The thickness of organic soil materials that overlie coarse textured glacial outwash is evident on this radar record from an area of Freetown soils in southwestern Massachusetts.

water are 1 and ~80, respectively. The permittivity of most mineral soils ranges from ~3 to 40, depending on soil water content. The permittivity of dry mineral soils ranges from 3 to 5. Several petrophysical models are available to convert measurements of dielectric permittivity to estimates of soil water content. One of the most commonly used models was developed by Topp et al. (1980). This empirical model was developed using a range of agricultural soils. Because the dielectric permittivity is the only input, the model can be easily applied to sites that have significant soil heterogeneity or limited soil characterization. Topp's empirical model for estimating soil water content (θ) from dielectric permittivity (K) is expressed as:

$$\theta = (5.3 \times 10^{-2}) + (2.29 \times 10^{-2})\mathrm{K} - (5.5 \times 10^{-4})\mathrm{K}^2 + (4.3 \times 10^{-6})\mathrm{K}^3 \qquad [1]$$

Other empirical relationships have been developed for different soil textures. Soil-specific empirical relationships can also be developed using data from GPR or a time domain reflectometer (TDR). Another type of petrophysical relationship uses the volume fraction and measured permittivity of each soil component (soil solids, air, and water). However, these volume-averaging relationships typically require porosity as an input, which may vary widely across a site and is often unknown (Roth et al., 1990).

Dielectric permittivity can be estimated from measurements of the electromagnetic velocity in most earthen materials. Unless the material is very electrically conductive, the dielectric permittivity depends only upon the velocity of the radar signal. In materials that have moderate

to low electrical conductivity, the relationship between the radar signal velocity (v) and dielectric permittivity (K) is:

$$K = (c/v)^2 \quad [2]$$

In equation 2, c is the speed of light (Conyers, 2004). Several methods are available for measuring velocity. The most common method uses reflected energy from a subsurface interface. If the depth to a subsurface reflector is known, the velocity may be calculated using the time needed for the energy to travel from the transmitter to the reflector and then back to the receiver. This travel time can be determined by the arrival time of a reflection viewed on a radar record. If the depth to a reflector is not known, the velocity can be obtained by performing a variable-offset survey. This method requires separate transmitting and receiving antennas. In a variable-offset survey, the transmitting and receiving antennas are initially placed close together and then incrementally moved further apart with each measurement. The velocity can be measured by analyzing the travel time of the reflected signal as a function of distance as the antennas are moved apart. Although variable-offset surveys provide important information on velocity and reflector depth, they are time-consuming and thus cannot be used to monitor large areas.

GPR reflection techniques can also be used to provide non-continuous measurements of velocity and thus soil water content. These measurements can be taken when a reflection hyperbola is created in the GPR record by isolated subsurface objects (e.g., stones and metal fragments) or by buried pipes that trend perpendicular to the GPR traverse. Reflection hyperbolas appear on GPR records as upside-down U shapes. Curve fitting procedures for reflection hyperbola can be employed to estimate the velocity. These procedures adjust a modeled shape to match the shape of the reflection hyperbola on a radar record. This fitting yields an estimate of the bulk soil radar velocity from the surface down to the isolated object or pipe. The depth to an isolated object or pipe does not need to be known in order to use this method. However, the visual fitting of the best curve to a reflection hyperbola is somewhat subjective and can lead to inaccuracies in velocity determination.

Another technique for estimating velocity uses the GPR groundwave. Groundwaves travel in the shallow subsurface (0 to ~30 cm) directly between the transmitting and receiving antennas. By noting the antenna separation and measuring the time needed for energy to travel between antennas, the velocity can be calculated. Groundwaves do not require a reflective interface and so can be applied in many soil environments. Because water content is commonly influenced by soil texture, groundwave measurements have also been used to map variations in

soil texture at the field scale (Grote et al., 2003). Some researchers (van Overmeeren et al., 1997; Galagedara et al., 2005; Grote et al., 2010) have also found that the groundwave sampling depth is frequency dependent. Multi-frequency groundwave data could therefore be used to map the shallow, three-dimensional distribution of water content.

In addition to reflection hyperbola and GPR groundwave, a third GPR technique for estimating water content in soil uses air-launched GPR to obtain reflections from the soil surface. In this technique, the magnitude of the reflection from the ground surface is used to measure the dielectric permittivity. Air-launched data can be acquired and processed quickly. However, the technique has a sampling depth of less than 5 cm and the accuracy of the data is greatly diminished by vegetation, uneven soil surfaces, and vertical variations in water content. As a result, this technique has limited applications (Serbin and Or, 2003).

Electromagnetic Induction (EMI)

Electromagnetic induction methods use ground conductivity meters (GCM). These meters consist of a transmitter coil and either a single receiver coil or multiple receiver coils that are spaced at prescribed distances. Ground conductivity meters generate alternating electrical currents that are passed through the transmitter coil. These alternating electrical currents generate a time-varying, primary electromagnetic field. This primary field induces eddy currents to flow through the soil and thereby generate a secondary electromagnetic field. The amplitude and phase of the primary and secondary electromagnetic fields are measured by the receiver coil(s). Under conditions known as "operating at low induction numbers" (McNeill, 1980), the secondary field is proportional to the ground current and is used to calculate the "apparent" or "bulk" electrical conductivity (EC_a) of the soil, which is commonly expressed in units of millisiemens per meter (mS/m).

Apparent electrical conductivity is a depth-weighted average measurement for a column of earthen materials to a specific depth (Greenhouse and Slaine, 1983). Variations in EC_a are produced by changes in the electrical conductivity of earthen materials. The electrical conductivity of soils is principally affected by the type and concentration of ions in solution, the amount and type of clays in the soil matrix, water content, and the temperature and phase of the soil water (McNeill, 1980). Apparent electrical conductivity increases with increases in concentration of soluble salts, content of water or clay, and temperature (McNeill, 1980). Although EMI has been principally used to map variations in EC_a, GCMs have also been used to map variations

in magnetic susceptibility—a property useful in delineating hydric soils and differences in some lithologies (Allred et al., 2010).

Modern GCMs are well suited to soil studies. Each GCM is fairly lightweight and can be operated in pedestrian or mobile modes (fig. 6-6). Because EMI does not require direct contact with the ground, data collection is relatively easy, rapid, and inexpensive. EMI therefore allows a larger number of measurements than traditional soil survey tools and more comprehensive coverage of sites. Electromagnetic induction has been used in order 1, 2, and 3 soil surveys to indirectly measure the spatial and temporal variability of soil properties. Examples include salinity, texture, cation-exchange capacity, ionic composition, $CaCO_3$ content, moisture content, organic carbon content, plant-available nutrients, pH, bulk density, and structure (Doolittle and Brevik, 2014).

The effectiveness of EMI depends on the degree to which differences in EC_a correspond to differences in the property under investigation. In general, stronger correlations are obtained where large differences in measured soil property and EC_a occur and other soil properties that affect EC_a remain relatively invariable. Differences can be horizontal, vertical, or both. Weaker correlations and lower predictive accuracies occur where the measured soil property and EC_a display low variability in relation to other interacting and more variable soil properties that affect EC_a. EC_a mapping is recognized as one of the most valuable methods in agriculture for measuring the spatial variability of soil properties at field and landscape scales (Corwin, 2008; Lück et al., 2009).

The depth of investigation (DOI) for EC_a measurements made with GCM is generally taken as the depth of 70 percent cumulative response. The DOI is dependent on the conductivity of the soil and the frequency, dipole orientation, and intercoil spacing of the GCM. For the GCMs most commonly used in soil investigations, the DOI can range from about 30 to 300 cm. DOIs from 3 to 60 m are possible with other commercially available GCMs.

Interpretations are commonly based on the identification of spatial patterns within EMI data sets. EMI was initially used to assess soil salinity, but its use has expanded to include mapping soil types; characterizing soil water content and flow patterns; assessing variations in soil texture, compaction, and organic matter content; and determining the depth to subsurface horizons, stratigraphic layers, or bedrock surfaces. Electromagnetic induction has also been used to assess differences in lithology and mineralogy, pH, field-scale leaching rates of solutes, herbicide partition coefficients, cation-exchange capacity, available nitrogen, and exchangeable Ca, Mg, and $CaCO_3$ (Doolittle and Brevik, 2014).

Figure 6-6

Three of the commercially available ground conductivity meters used in soil investigations. Each has its own strengths and weaknesses. Pedestrian (left images) or mobile (right images) surveys can be conducted with each.

Advantages of EMI include its noninvasiveness, fast operating speed, and continuous recording of georeferenced data. The large amounts of georeferenced data that can be rapidly and inexpensively collected with EMI provide more complete characterization of the variability in soil properties at intermediate scales than traditional point-sampling methods. Electromagnetic induction does have limitations: results are

indirect, semi-quantitative, and site specific and vary depending on the complexity of the interactions that occur among multiple and varying soil properties. In addition, sferics (magnetic impulses from lightning) and nearby power sources and metal objects can interfere with and degrade the quality of EMI measurements. Limited ground-truth information and knowledge of the soils and the sources of EC_a variation are required to properly interpret data.

Examples of EMI Use in Soil Survey

Figure 6-7 shows the spatial variability of EC_a across a 7.7-ha range site that includes a portion of a dried-up playa bed in northern Texas. The very deep, poorly drained Randall soils (very-fine, smectitic, thermic Ustic Epiaquerts) formed in clayey lacustrine sediments on the playa floor. The very deep, well drained Olton soils (fine, mixed, superactive, thermic Aridic Paleustolls) formed in loamy, calcareous, eolian sediments on the slopes that surround the playa. At this site, variations in EC_a are principally associated with differences in soil moisture and clay content. Areas of higher EC_a (> 36 mS/m) were associated with the finer textured (> 50% clay), more imperfectly drained Randall soils.

On the EC_a map in figure 6-7, soil variability and the transition from one soil type to another are well expressed. The soil map unit boundary line was imported from Web Soil Survey (Soil Survey Staff, 2015). This boundary has a fixed width and cannot accurately portray the spatial rate of change or the complex spatial variability of soils and soil properties along the transition between playa and upland. As evident on this map, spatial EC_a data can improve the placement of the soil boundary line and the representation of soil variability.

Figure 6-8 is an EC_a map of a 4.5-ha pasture in northeastern Iowa. Across this field, the surface slopes down to the north and northwest. The highest elevation is in the southeast corner of the field. The soil boundary lines were imported from the Web Soil Survey (Soil Survey Staff, 2015). In figure 6-8, the names of the dominant soil for each consociation are shown. These very deep soils all formed in loamy sediments overlying loamy till but belong to different soil drainage classes. Ostrander soils (fine-loamy, mixed, superactive, mesic Typic Hapludolls) are well drained; Kasson soils (fine-loamy, mixed, superactive, mesic Oxyaquic Hapludalfs) and Marquis soils (fine-loamy, mixed, superactive, mesic Oxyaquic Hapludolls) are moderately well drained; Floyd soils (fine-loamy, mixed, superactive, mesic Aquic Pachic Hapludolls) are somewhat poorly drained; and Clyde soils (fine-loamy, mixed, superactive, mesic Typic Endoaquolls) are poorly and very poorly drained.

Figure 6-7

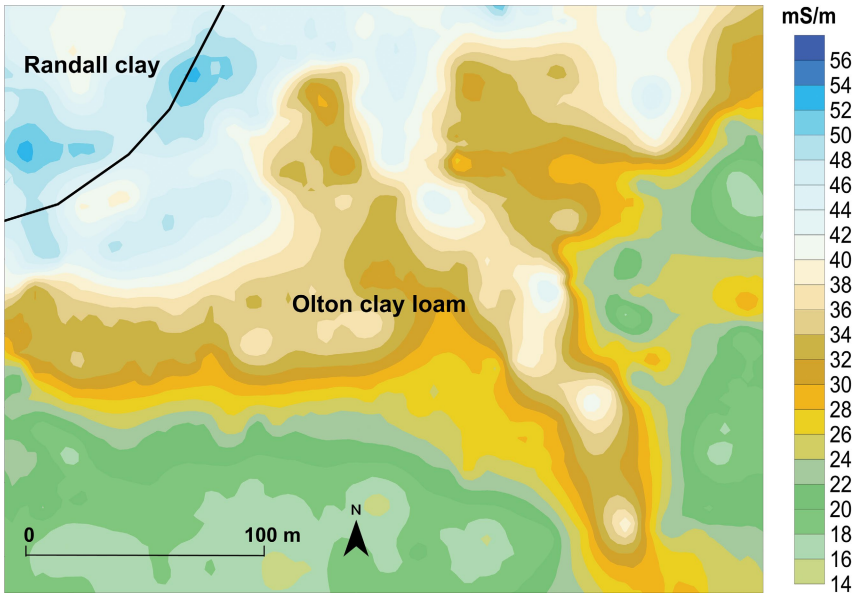

Spatial variations in EC_a within the upper 150 cm of the soil profiles at a site in northern Texas. This information was used to improve the placement of boundary lines and the characterization of soils. The map unit names and the soil boundary line were imported from the Web Soil Survey.

Figure 6-8

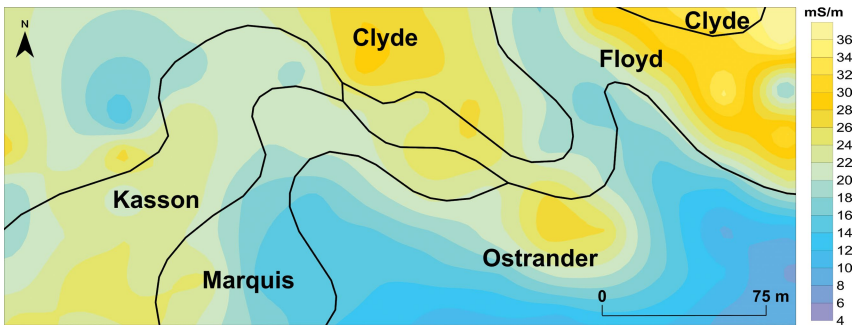

Spatial variations in EC_a within the upper 150 cm of five soils in northern Iowa. These variations are attributed principally to differences in soil drainage class and moisture content. Soil names and boundary lines were imported from the Web Soil Survey.

The complex spatial patterns evident on the high-intensity EC_a map in figure 6-8 principally reflect differences in soil drainage class and moisture content. In the northern portion of the field, areas of high conductivity (> 24 mS/m) closely mimic the distribution of the wetter, more imperfectly drained Clyde and Floyd soils. Areas of lower EC_a (< 20 mS/m) correspond with the higher-lying, better drained Ostrander soils, which are on convex surfaces that dominate the southeastern portion of the field. Areas of higher conductivity that extend northwest to southeast are associated with draws situated between higher-lying ridgelines. Apparent conductivity maps, such as figure 6-8, help reveal the complexity of soil-landscape architectures and their impact on subsurface flow and soil moisture patterns at field scales.

Figure 6-9 shows the spatial variability of EC_a within the upper 150 cm of a soil that contains saline seeps. The 64.7-ha field is in north-central Montana. The soil map unit boundary lines were imported from the Web Soil Survey (Soil Survey Staff, 2015). The soils are Megonot (fine, smectitic, frigid Torrertic Haplustepts), Pylon (fine, smectitic, frigid Torrertic Haplustalfs), and Tanna (fine, smectitic, frigid Aridic Argiustolls). These moderately deep, well drained soils formed in residuum weathered from semi-consolidated shale and siltstone. The presence of saline seeps is largely controlled by surface geology, above-normal periods of precipitation, and farming practices that help water to move beyond the root zone. As excess water moves through the soil, it dissolves water-soluble minerals. When an impermeable layer is encountered, the downward flow of water is restricted and redirected laterally along the restricting layer into lower-lying slope positions. Saline seeps develop wherever the saline ground water comes within about 1.5 m of the surface (Daniels, 1987).

In figure 6-9, the saline seeps are identified by their high EC_a (> 170 mS/m). These seeps are arranged in a discontinuous, sinuous pattern. They meander across the field from the southwest to the northeast along the base of slopes. This plot also shows lines of moderate EC_a that extend upslope away from the seeps. The areas of high EC_a represent discharge areas for subsurface flow where dissolved salts concentrate when water is lost by evapotranspiration. Recharge areas for the subsurface flow are located upslope from the saline seeps (to the west and north) and have relatively low EC_a (< 85 mS/m).

Electrical Resistivity (ER)

Soil electrical resistivity represents the capacity of soil materials to resist the flow of electrical current. Methods that calculate the apparent

Figure 6-9

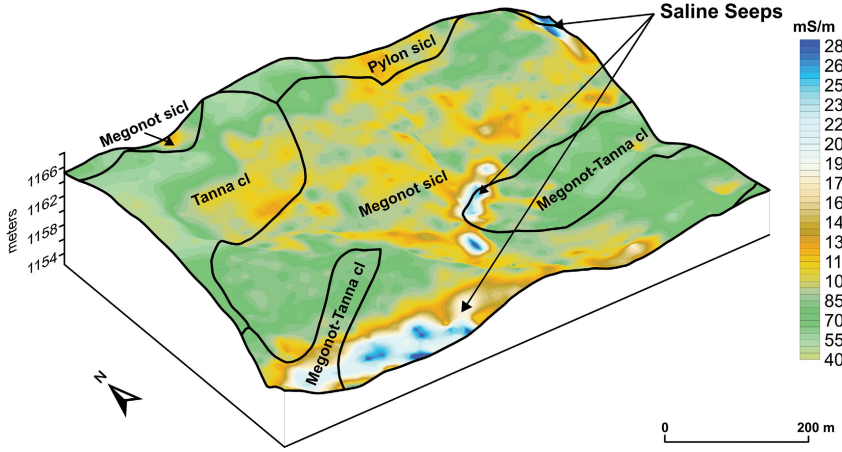

Spatial distribution of EC_a across a cultivated field in north-central Montana. Spatial EC_a patterns provide inferences about flow of subsurface water and soluble salts across this landscape and about the distribution of recharge, discharge, and flow-through areas that contribute to the development of saline seeps. Soil names, surface textures, and boundary lines were imported from the Web Soil Survey.

electrical resistivity use Ohm's law and the measured injected current, the measured potential difference, and a geometric factor. The geometric factor is a function of the electrode spacing or configuration (Samouëlian et al., 2005). Apparent resistivity is commonly expressed in units of ohm-meters (Ωm). The apparent resistivity is a complex function of the composition and arrangement of solid soil constituents, porosity, pore-water saturation, pore-water conductivity, and temperature (Samouëlian et al., 2005). Electrical resistivity methods can be divided into those that inject currents into the ground through direct coupling and those that inject through capacitively induced coupling. Typically, both types of methods measure the apparent electrical resistivity, which is subsequently converted to its inverse, the apparent electrical conductivity of the soil.

Direct-Coupling ER

The traditional direct-coupling electrical resistivity method, also known as the galvanic source method, injects electrical current into the soil using an array of electrodes that are in contact with the ground. In a common four-electrode array, an electrical current is applied between two "current" electrodes and the voltage (the electric potential difference) is measured between two "potential" electrodes. For field surveys, current

and potential electrodes are maintained at a fixed distance from each other. The array is moved along a survey line to successive measurement points. Horizontal and vertical resolution, depth of investigation, and signal-to-noise ratio vary with the configuration of the electrode array (Samouëlian et al., 2005). The depth of investigation and volume of soil materials measured increase with increasing electrode spacing. Conversely, resolution decreases with increasing electrode spacing. Depending on the relative positioning of the potential and current electrodes, several different array configurations are possible. The three most common configurations are the Schlumberger, Wenner, and dipole-dipole (Allred et al., 2008b). The Wenner array is more sensitive to mapping lateral changes in electrical resistivity. The Schlumberger and dipole-dipole arrays are often preferred for vertical soundings that measure variations in apparent resistivity with depth (Allred et al., 2008b; Samouëlian et al., 2005).

In many investigations, ER data are inverted. Inversion is an iterative process that results in a 2D or 3D model of the subsurface that best fits the acquired data. However, models constructed from inverted data provide nonunique solutions. Models are nonunique because, based on the constraints applied during the inversion process, several solutions or representations of the same data set are possible.

Apparent electrical resistivity has been used in order 1, 2, and 3 soil surveys to indirectly measure and characterize variations in soil structure and physico-chemical properties, detect preferential flow paths, and monitor temporal changes in soil water distributions. As noted by Samouëlian et al. (2005), electrical resistivity allows the delineation of soil types and, when performed repeatedly over time, provides information on soil functioning.

Standard ER surveys, which require the repetitive insertion and removal of electrodes from the soil, are relatively labor-intensive and time-consuming. To reduce survey time, computer-controlled, multi-electrode systems with tens to hundreds of electrodes have been developed (Allred et al., 2008b). These systems, however, have had limited use in soil studies.

Highly mobile, continuously recording, towed-array ER systems have been developed to expedite fieldwork and facilitate the collection of spatially dense data sets at field scales. In the United States, towed electrode-array ER systems have been used in precision agriculture and soil research (fig. 6-10). A commonly used system has six coulter-electrodes (two current and four potential electrodes) with nonadjustable spacing (Veris Technologies, 2016). It is configured in a modified Wenner array (Sudduth et al., 2005) and programed to simultaneously map EC_a

over two soil depth intervals (i.e., 0 to 30 cm and 0 to 90 cm) (Lund et al., 2000). Other systems use a single adjustable array to map EC_a within the top 45 to 90 cm of the soil profile. Both systems are preprogrammed and do not need calibration. In addition, unlike EMI sensors, measurements are not affected by sferics (electromagnetic pulses caused by atmospheric phenomena) or by nearby metallic objects, utility wires, or engines. However, towed-electrode arrays are invasive so their field use is commonly restricted by plant growth and cover and soil wetness. As soil contact must be maintained at all times during mapping, these systems should be operated neither on frozen or rocky soils nor in some bedded or furrowed cultivated fields.

Figure 6-10

A towed electrode-array (six coulter-electrodes) soil EC_a mapping system behind a utility vehicle in a field of corn stubble.

Example of Direct-Coupling ER Use in Soil Survey

Figure 6-11 shows the results of a high-intensity survey conducted across a 32.4-ha field in western Illinois. Soil names, map unit symbols, and boundary lines from a high-intensity soil survey are shown on the plot of the deep (0 to 90 cm) data (image on right). Only the boundary lines are shown on the plot of the shallow (0 to 30 cm) data (image on left). The soils are very deep Mollisols that formed in thick loess deposits

and belong to the fine-silty and fine particle-size classes. Although they belong to different particle-size classes, the soils do not vary appreciably in clay content. They range from poorly drained Aquolls to somewhat poorly drained and moderately well drained Udolls. Major soils identified within the study site are Ipava, Buckhart, Edinburg, and Sable soils. The somewhat poorly drained Ipava soils (fine, smectitic, mesic Aquic Argiudolls) and the moderately well drained Buckhart soils (fine-silty, mixed, superactive, mesic Oxyaquic Argiudolls) are in upland areas. The poorly drained Sable (fine-silty, mixed, superactive, mesic Typic Endoaquolls) and Edinburg soils (fine, smectitic, mesic Vertic Argiaquolls) are along intermittent drainageways and in broad summit areas, respectively.

Figure 6-11

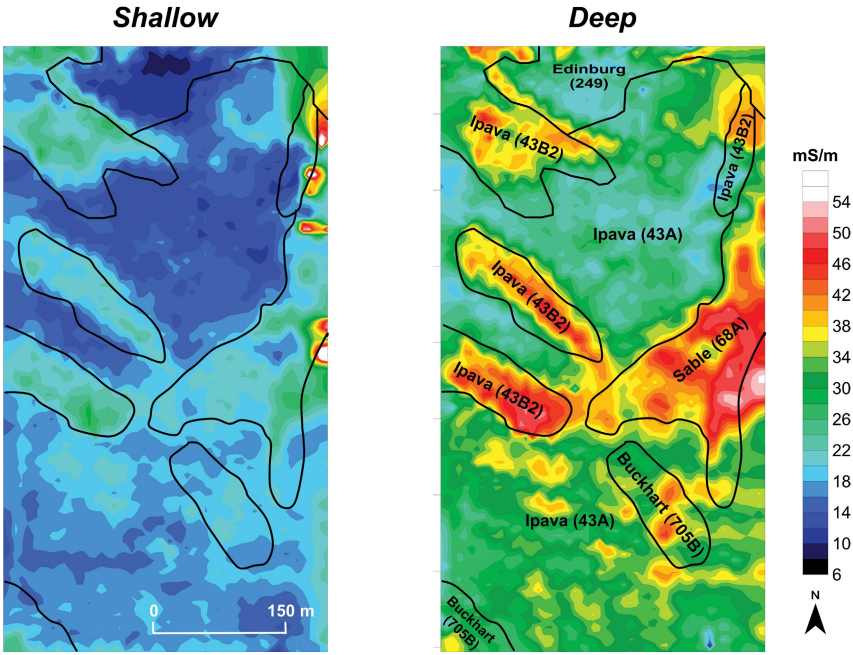

Maps of apparent conductivity prepared from shallow and deep data collected in west-central Illinois.

In figure 6-11, the EC_a is noticeably lower in the shallow (0 to 30 cm) map than in the deep (0 to 90 cm) map. This is due to the increase in clay and water contents in deeper horizons. For the deep measurements, areas with lower EC_a represent better drained, higher-lying areas of Ipava and Buckhart soils. Higher EC_a values were measured in the more

sloping and eroded areas of Ipava soils (43B2) where the argillic horizon is shallower and seepage was observed. Lower-lying areas of Sable soils are wetter and have a higher EC_a. In the southern portion of the field, on the deep map, faint patterns of three parallel, essentially east-west-trending terraces can be identified by their higher EC_a.

Capacitively Induced Coupling

Capacitively induced coupling resistivity (CCR) systems use capacitive coupling rather than galvanic contact to introduce electric current into the ground. They measure voltage at the surface in order to determine apparent soil electrical resistivity. The capacitive coupling uses coaxial cables to form a large capacitor. The metal shield of the coaxial cable is one of the capacitor plates and the soil surface is the other. The outer insulation of the coaxial cable acts as the dielectric material separating the two plates. The system transmitter applies an alternating current (AC) to the coaxial cable side of the capacitor, which in turn generates AC in the soil on the other side of the capacitor. With regard to the receiver, a similar phenomenon occurs, except in reverse. The AC in the soil charges the receiver coaxial cable capacitor, and the measured capacitance is then used to determine the potential difference (voltage) generated by the flow of electric current within the soil.

One of the more common CCR systems has two coaxial cables attached to the transmitter, one on each side, to form a current dipole, and it has two coaxial cables attached to the receiver, one on each side, to form a potential dipole (Geometrics, 2001). The depth of investigation for the system is 0.1 to 20 m, depending on dipole cable and tow-link length. This set-up, along with some initial data processing, allows this CCR system (fig. 6-12) to mimic a conventional galvanic contact dipole-dipole electrode array. A conventional array consists of one pair of current electrodes (current dipole) and one pair of potential electrodes (potential dipole). By increasing the distance between the receiver and transmitter dipoles, the depth of investigation and volume of soil measured are increased (Walker and Houser, 2002). Inverse modeling methods can be employed to produce depth profiles of electrical conductivity (fig. 6-13) if CCR data are collected along a transect line using several different spacing distances between transmitter and receiver dipoles.

Capacitively induced coupling resistivity systems are rarely used in soil studies. In the field, the lines are easily snared on obstacles and broken off (Gebbers et al., 2009). CCR systems work exceedingly well in high resistivity soils, where it is often difficult to transfer sufficient current into the ground with towed-electrode array systems. In highly conductive soils, however, these systems provide little signal penetration and the resulting data are noisy (Gebbers et al., 2009).

Figure 6-12

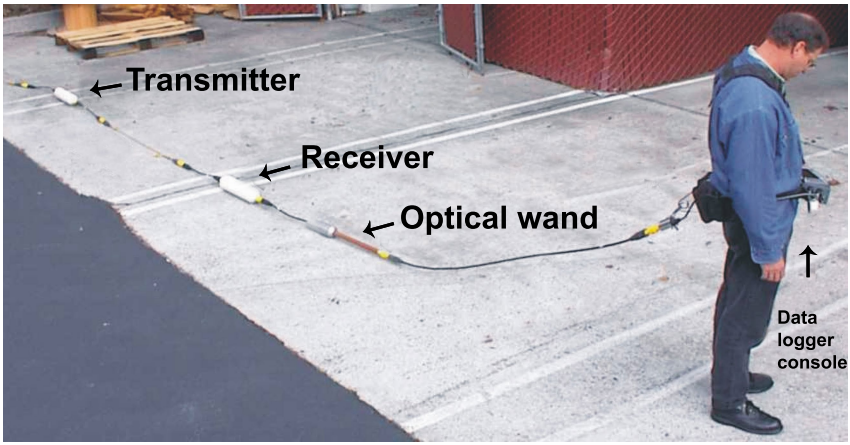

A common capacitively induced coupling resistivity system. (Photo courtesy of Geometrics, Inc.)

Figure 6-13

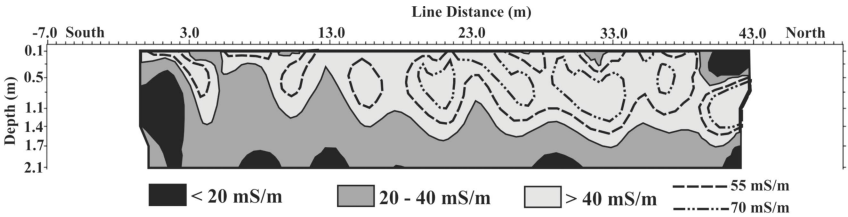

A soil electrical conductivity depth profile from an agricultural test plot at the Ohio State University in Columbus, Ohio. The data for this profile were collected using spacing distances of 0.625 m, 1.25 m, 2.5 m, and 5 m between receiver and transmitter dipoles. To generate the soil electrical conductivity profile shown, data were input to a two-dimensional, least-squares optimization, inverse computer modeling program developed by Loke (2014).

Less Common Proximal Sensing Methods

The proximal sensing methods that are less commonly used by the National Cooperative Soil Survey include magnetometry, magnetic susceptibility, portable X-ray fluorescence, time domain reflectometry,

optical reflectance, gamma-ray spectroscopy, mechanical interactions, ion-selective potentiometry, and seismic.

Magnetometry (MT)

Magnetometry is a passive remote sensing method that records the magnitude of the Earth's local magnetic field. Its sensors, called magnetometers, may be placed on the ground surface, in the air, in satellites, or in boreholes beneath the surface of the Earth. For measurements in agricultural fields, magnetometers are typically positioned within a couple of meters of the ground surface. Gradiometers, which are better adapted to emphasize magnetic field anomalies from shallow sources, are set up with two magnetometers mounted a short distance (< 1 m) apart. This arrangement allows the magnetic field gradient between them to be measured (fig. 6-14). Gradiometers have the added advantage of eliminating the need to make corrections for diurnal fluctuations in the magnetic field. Magnetic surveys using gradiometers have successfully found disturbances (e.g., backfilled trenches and excavated areas) in

Figure 6-14

Magnetic surveying with a cesium vapor gradiometer (Geometrics, 2016) integrated with a global positioning system receiver (Trimble, 2016).

iron-rich soils (Rogers et al., 2005). This suggests the potential use of this technology to identify the extent and location of some anthropogenic soils, particularly in order 1 soil survey applications.

Magnetic Susceptibility (MS)

Magnetic susceptibility is a measure of the degree to which a material can be magnetized when subjected to an applied magnetic field. The magnetic susceptibility of soil depends on the concentration, size, and shape of strongly magnetic minerals as well as the method of measurement (Mullins, 1977). Strongly magnetic minerals include ferromagnetic minerals, such as magnetite, maghemite, titanomagnetite, and pyrrhotite. Sources of MS can be lithogenic, pedogenic, or anthropogenic (Grimley et al., 2004). In soils, MS is influenced by differences in parent material, soil age, texture, mixing, firing, weathering, additions to the soil (commonly anthropogenic), pH, organic matter content, and soil moisture content (Maier et al., 2006; Grimley et al., 2004; Mullins, 1977).

Handheld susceptibility meters allow MS measurement across soil surfaces, down small-diameter holes, and on exposed sections (e.g., Bartington, 2016). These single-coil sensors require direct contact with the soil, and their depth of investigation is related to the diameter of the coil. The effective penetration depth of most handheld susceptibility sensors is limited to about 1 to 10 cm. Borehole sensors, however, can document vertical contrasts in susceptibility to depths as great as 20 m (Dalan, 2006). Unlike GPR, EMI, and ER, magnetic susceptibility surveys are not significantly affected by variations in soil moisture content. Because the volumes that are measured by MS sensors are small, high spatial resolution can be achieved. However, the accuracy of handheld, single-coil MS sensors is diminished by thermal drift and in areas that have rough, rocky surfaces or thick vegetation.

Magnetic susceptibility can also be measured with ground conductivity meters (GCM). The inphase component of the secondary electromagnetic field in a GCM is considered proportional to, and has been used to map, variations in magnetic susceptibility. However, the inphase response of an EMI sensor is more restricted by depth than the quadrature phase response (apparent conductivity). The inphase response of a commonly used meter measures only the top 50 cm of soil (Dalan, 2006). Interpretations of magnetic susceptibility from EMI data are also challenging. Variations are caused by differences in instrument configuration, instrument height and orientation, surface topography and roughness, depth to target, and changes in the sign (±) of the response in relation to target depth (Shamatava et al., 2007; Tabbagh, 1986). Other

drawbacks of EMI sensors include instrument drift and the use of an arbitrary zero level.

Results of MS surveys are displayed as individual profiles or contour plots. Typically, field measurements of MS are reported in dimensionless volume units, e.g., 10^{-5} (SI) (Mullins, 1977).

Where sufficient contrast in magnetic properties exists, MS has been associated with pedogenesis (Fine et al., 1989), gleying (Vadyunina and Babanin, 1972), slope position (De Jong et al., 2000), soil drainage class and texture (Grimley et al., 2004), human disturbances (Dalan and Banerjee, 1996), and industrial pollutants (Fialová et al., 2006; Magiera et al., 2006). Where the concentration of magnetic minerals is sufficiently high, MS has been used to delineate boundaries of hydric soils (Lobred and Simms, 2009; Zwanka et al., 2007; Grimley et al., 2004; Arruda and Grimley, 2002; Grimley and Vepraskas, 2000) and to differentiate soil types (Hanesch and Scholger, 2005; Dearing et al., 1996; Vadyunina and Smirnov, 1978). Magnetic susceptibility is most applicable to some order 1 soil surveys.

Portable X-Ray Fluorescence (P-XRF)

Portable X-ray fluorescence spectrometers use high-energy incident X-ray photons to forcibly eject electrons from the inner shell of atoms. The resulting electron holes cause instability, which causes electrons from the outer shell to drop into the inner shell and fill the voids. This process results in the emission of X-ray energy, which is referred to as X-ray fluorescence. Because the energy emitted as fluorescence is element specific, different elements can be identified and quantified (Weindorf et al., 2012a). A comprehensive discussion of P-XRF is provided by Kalnicky and Singhvi (2001). Soil samples and exposed surfaces can be readily scanned with P-XRF spectrometers (fig. 6-15).

X-ray fluorescence has been principally used to assess metals in contaminated soils (Dao et al., 2012; Schwarz et al., 2012; Weindorf et al., 2012b; Kalnicky and Singhvi, 2001). Weindorf et al. (2012a) used P-XRF to improve descriptions of soil morphology and differentiate soil horizons based on the concentration of different metals. In gypsiferous soils of west Texas, Weindorf et al. (2009) used P-XRF to quantify the calcium content and determine the percent of gypsum. Beaudette et al. (2009) conducted P-XRF surveys in two watersheds, one formed over metavolcanic rocks and the other over granite. They used the resulting geochemical data to infer differences in soil development weathering indices, mineralogy, and geologic signatures. Doolittle et al. (2013) used EMI and P-XRF data to characterize differences in the mineralogy

and lithologies of serpentinite- and non-serpentinite-derived soils in the Northern Piedmont of Pennsylvania. In soil survey, P-XRF is primarily applicable to point data documentation.

Figure 6-15

A portable XRF spectrometer, which can be attached to a monitoring bench in an office to scan collected samples (left) or can be used in the field to scan exposed faces of soil pits or surfaces (right).

Time Domain Reflectometry (TDR)

Time domain reflectometry (TDR) measures soil water content and, with some sensors, electrical conductivity. The use of TDR in soil science was pioneered by Topp, Davis, and Annan (1980). TDR infers water content and electrical conductivity from the measured dielectric permittivity and signal attenuation, respectively (Jones et al., 2002).

With TDR, a waveguide, or probe, of known length is inserted into the soil and the travel time for a generated electromagnetic pulse to traverse this length is measured. Using empirical (Topp et al., 1980; equation 1) or dielectric mixing models, the travel time is converted into a velocity of pulse propagation. The velocity of propagation is used to determine the soil's bulk dielectric permittivity, which is used to infer the volumetric water content. The dielectric permittivity is directly related to soil volumetric water content.

According to Jones et al. (2002), some of the advantages of TDR are: (1) accurate estimations of soil volumetric water content (to within ± 2% without soil-specific calibration), (2) minimal calibration requirements

in most soils, (3) absence of radiation hazards that are associated with neutron probe or gamma-attenuation techniques, (4) excellent spatial and temporal resolution, and (5) ease of measurements. Some of the disadvantages of TDR are: (1) measurement errors can occur if there are gaps between the soil and probe, (2) TDR is limited in highly saline and frozen soils (Ferrara and Flore, 2003), (3) special calibrations are required in soils that have a high content of clay or organic matter content, and (4) probes are difficult to insert in some soils.

A variety of TDR sensors are available for determining water content in soil. Depending on the length of the waveguide, TDR sensors can provide bulk soil moisture measurements over different soil depths. In soil survey, time domain reflectometry is primarily applicable to point-data documentation.

Optical Reflectance (UV, vis-NIR, mid-IR)

Optical sensors are used to determine the soil's ability to reflect light in different parts of the electromagnetic spectrum. Proximal optical sensors are fundamentally the same as remote sensing systems. The advantage of proximal sensors is that they can be applied at the surface and below ground (fig. 6-16). In soil survey, optical reflectance is applicable to point data documentation. It can be used for on-the-go measurements during different soil survey practices. In addition, both near and mid infrared diffuse reflectance spectroscopy are being used in the laboratory for rapid determination of some soil properties. Optical sensing systems cover the ultraviolet (100–400 nm), visible (400–750 nm), near infrared (750–2,500 nm), or mid infrared (2,500–25,000 nm) wavelengths or a combination of these wavelengths. Typically, instruments used for soil measurements include their own light source (e.g., a light bulb or light-emitting diode). Photodiodes or array detectors are used to estimate the intensity of reflected light and relate this measure to the light reflected from a given set of standards. Both source and reflected light can be transmitted through the air, via fiber optics, or when feasible, through a contact window fabricated from highly resistive material, such as sapphire or quartz.

Measurements obtained using optical sensors can be related to a number of soil attributes, such as soil mineral composition, clay content, soil color, moisture, organic carbon content, pH, and cation-exchange capacity (Christy, 2008; Viscarra Rossel et al., 2009; Mouazen et al., 2010). Measurements can be direct or indirect. For direct measurements, relationships are based on a physical phenomenon that affects light reflectance in a specific part of the spectrum (e.g., soil mineralogy or

Figure 6-16

A probe equipped with insertion load sensors and two spectrometers, which cover visible and near infrared parts of the spectrum as well as electrical conductivity.

water content is predicted using water absorption bands). For indirect measurements, relationships are deterministic for a finite domain and the combined effects of several soil attributes can be related to a given soil characteristic (e.g., soil organic matter). Sensor calibration strategies range from a simple linear regression to multivariate methods, chemometrics, and data mining (Viscarra Rossel et al., 2006). Although some of these models may be applied to large geographic areas, most are currently associated with a specific range of soils.

Ultraviolet (UV) radiation has been used in combination with visible or infrared spectra (e.g., Islam et al., 2003). Ultraviolet and visible spectra have been used to characterize inorganic minerals, such as iron oxides (Schwertmann and Taylor, 1989). An extensive range of reports is available on the use of visible near infrared (vis-NIR) and mid infrared (mid-IR) spectra for soil analysis. Both laboratory conditions and proximal soil sensing have been investigated. The mid-IR contains more information on soil mineral and organic composition than the vis-NIR, and its multivariate

calibrations are generally more robust. The mid-IR has these advantages because fundamental molecular vibrations of soil components occur in the mid-IR while only their overtones and combinations are detected in the vis-NIR. Thus, soil vis-NIR spectra display fewer and much broader absorption features compared to mid-IR spectra.

Gamma-Ray Spectroscopy

Gamma rays contain a very large amount of energy and are the most penetrating radiation from natural or artificial sources. Gamma-ray spectrometers measure the distribution of the intensity of gamma (γ) radiation versus the energy of each photon. Sensors may be either active or passive. Active γ-ray sensors use a radioactive source (e.g., cesium-137) to emit photons of energy that can then be detected using a γ-ray spectrometer (e.g., Wang et al., 1975). Passive γ-ray sensors measure the energy of photons emitted from naturally occurring radioactive isotopes of the element from which they originate (e.g., Viscarra Rossel et al., 2007). Soil elemental isotopes can be mapped by a γ-ray sensor on a vehicle (fig. 6-17). Data interpretation may include analysis of measures related to the isotopes of potassium, thorium, and uranium or the total count. Such mapping can be a useful tool for predicting soil properties in different soil landscapes. A significant amount of preprocessing, however, is commonly required to reveal relationships between the γ-ray spectra and the soil data (Viscarra Rossel et al., 2007). In soil survey, gamma-ray spectroscopy is primarily applicable to order 1 surveys (and possibly some order 2 or 3) as well as to point-based measurements.

Figure 6-17

A vehicle-mounted passive gamma-ray sensor.

Inelastic neutron scattering (INS) spectroscopy (Schrader and Stinner, 1961) relies on the detection of γ-rays that are emitted following the capture and reemission of fast neutrons as a sample is bombarded with neutrons from a pulsed neutron generator. The emitted γ-rays are characteristic of the excited nuclide, and the intensity of γ-rays is directly related to the elemental content of the sample. The detectors used are the same as those used in γ-ray spectroscopy. Wielopolski et al. (2008) proposed the use of INS spectroscopy for the measurement of carbon and other elements in soils.

Mechanical Interactions

Simple mechanical sensors can be used to estimate soil mechanical impedance (resistance). By nature, these soil strength sensors measure resistance to soil failure (Hemmat and Adamchuk, 2008). As a mechanical resistance sensor moves through the soil, it registers resistance forces arising from the cutting, breakage, and displacement of soil, as well as from the parasitic (frictional and adhesive) forces that develop at the interface between the sensor's surface and the surrounding soil. Normally, soil mechanical resistance is expressed in units of pressure and represents the ratio of the force required to penetrate the soil media and the frontal (normal to the direction of penetration) area of the tool engaged with the soil.

The first step toward soil mechanical resistance sensing is to map the total horizontal (draft) force and, in some cases, the total vertical force applied to a traditional fixed-depth implement engaged with the soil. Recorded measurements represent surrogate values affected by a variety of factors, including the type and shape of the tool working the soil, the speed and depth of the operation, and the surface conditions. In addition to vertically operated cone penetrometers, horizontal sensors have been designed to generate high-resolution maps of horizontal soil penetration resistance obtained at a specific depth. Multiple tips can be simultaneously deployed at different depths. Such an arrangement allows researchers to determine the spatial variability of soil mechanical resistance at any available depth as well as vertical variability in each location of the field.

To avoid the expense of adding direct load-sensing tips, a single-tip horizontal sensor can be actuated vertically in a way similar to a bulk soil strength sensor. In addition to using a tip-based method, the vertical distribution of soil mechanical resistance can be measured using an instrumented tine. This distribution is measured by sensing the direct load applied to the tine at discrete depths and/or by measuring the degree of

bending using strain gauge technology (i.e., a cantilever beam approach). Maps of soil mechanical resistance corresponding to a 20–30 cm depth layer can reveal the appearance of old infrastructure, such as roads. Soil mechanical impedance changes with soil water content and bulk density. On-line soil moisture sensors (typically capacitance or near-infrared reflectance probes) have been used to separate these two soil attributes.

Acoustic and pneumatic sensors can be alternatives to mechanical sensors for the study of the interaction between soil and an agricultural implement. Acoustic sensors have been used to determine soil texture, bulk density, or both by measuring the change in the level of noise caused by the interaction of a tool with soil particles. Pneumatic sensors have been used for on-the-go sensing of air permeability in soil. The pressure required to force a given volume of air into the soil at a fixed depth was compared to several soil properties, such as soil structure and compaction. In soil survey, mechanical interactions are primarily applicable to order 1 surveys and point data documentation.

Ion-Selective Potentiometry

Ion-selective potentiometry sensor systems resemble a traditional wet-chemistry method to assess the content of certain chemical ions and compounds. They can provide the most important type of information needed for precision agriculture—soil nutrient availability and pH. The measurements are conducted using either an ion-selective electrode (ISE) or an ion-selective field effect transistor (ISFET). These sensors detect the activity of specific ions at the interface between sensitive membranes and the aquatic part of either a soil solution or a naturally moist sample. A common ISE system consists of a membrane that is sensitive to specific ions and a reference electrode. The difference in the potential between the sensitive membrane and the reference is measured and converted to the activity of specific ions in the tested solutions. The design of a combination ion-selective electrode allows both sensitive and reference parts to be assembled in one probe. Different electrode brands represent different designs of ion-selective membranes and reference junctions.

An ISFET integrates the ion-selectivity of an ISE with the small size and the robust nature of a field effect transistor. The current between two semiconductor electrodes (source and drain) is controlled by a gate electrode represented by an ion-selective membrane. As ions of interest affect the gate, their charge impacts the source-drain current, which provides an indication of ion activity. The main differences between an ISFET and an ISE are that an ISFET does not contain an internal solution and the ion selective membrane is affixed directly on the gate surface of

the ISFET. ISFET technology is attractive because of its compact size and theoretically high signal-to-noise ratio, especially when used for the flow injection analysis (FIA) method. However, the range of commercially available ISFETs remains relatively narrow. The sensitive membrane in both ISE and ISFET is made of glass (H^+, Na^+), polyvinyl chloride (K^+, NO_3^-, Ca^{2+}, Mg^{2+}), or metal (H^+).

A range of approaches can be used to establish the interface between an ISE or ISFET and a soil solution. Some methods involve great detail; some are relatively simple. On one end of the range of possibilities is a complete sample preparation with a prescribed controlled ratio between soil particles and extracting solution. This method adds complexity to the measurement apparatus and often requires a longer sampling time and analysis cycle (Viscarra Rossel et al., 2005). On the other end is a direct, simple measurement (DSM) approach, which is relatively easy to implement (Adamchuk et al., 2005). The real-time chemical extraction of the ions mimics conventional soil analysis procedures. DSM-based measurements reveal specific ion content in a given soil state, which may not represent nutrient availability throughout the growing season. Because chemical processes in soil are frequently influenced by the physical composition of the soil, combining direct ion activity measurements with geophysical instruments (described earlier) can help predict conventional laboratory test values used to prescribe various soil amendments (fig. 6-18). In soil survey, ion-selective potentiometry is primarily applicable to order 1 surveys and point data documentation.

Figure 6-18

A sampling mechanism for a towed system that simultaneously maps soil pH and apparent electrical conductivity.

Seismic

Seismic waves are essentially elastic vibrations that propagate through soil and rock materials. Artificial energy sources can be used to introduce seismic waves into the ground for investigatations of subsurface conditions or features. Examples of energy types include explosive, impacting, vibratory, and acoustic. For seismic geophysical methods in which artificial energy is supplied, the seismic waves are timed as they travel through the subsurface from the energy source to the sensors, which are called geophones. Incoming seismic wave amplitudes, and hence energy, are also measured at the geophones. The energy source is ordinarily positioned on the surface or at a shallow depth, and the geophones are typically inserted at the ground surface. Data on the timed arrivals and amplitudes of the seismic waves measured by the geophones provide insight into belowground conditions or help to characterize and locate subsurface features.

Traditional seismic methods have rarely been used for agricultural purposes. However, laboratory studies employing 2 to 7 kHz acoustic-sourced seismic waves have shown that seismic wave velocities correlate significantly with soil compaction, soil porosity, and soil water content and that acoustic-sourced seismic wave absorption coefficients exhibit significant correlation with soil bulk density and soil water content (Oelze et al., 2002; Lu et al., 2004). In the Appalachian Highlands Physiographic Province of northwestern Virginia, Olson and Doolittle (1985) used seismic refraction to determine the elevation of the water table and depth to bedrock. They noted, however, that this geophysical method could not distinguish soil profile characteristics. Seismic tools are potentially applicable in order 1, 2, or 3 soil surveys.

References

Adamchuk, V.I., and R.A. Viscarra Rossel. 2011. Precision agriculture: Proximal soil sensing. *In* J. Gliński, J. Horabik, and J. Lipiec (eds.) Encyclopedia of agrophysics, Springer, New York, NY, pp. 650–656.

Adamchuk, V.I., E. Lund, B. Sethuramasamyraja, M.T. Morgan, A. Dobermann, and D.B. Marx. 2005. Direct measurement of soil chemical properties on-the-go using ion-selective electrodes. Computers and Electronics in Agriculture 48(3):272–294.

Adamchuk, V.I., R.A. Viscarra Rossel, K.A. Sudduth, and P. Schulze Lammers. 2011. Sensor fusion for precision agriculture. *In* C.

Thomas (ed.) Sensor fusion–Foundation and applications, chapter 2, InTech, Rijeka, Croatia, pp. 27–40.

Allred, B.J., M.R. Ehsani, and J.J. Daniels. 2008a. General considerations for geophysical methods applied to agriculture. *In* B.J. Allred, J.J. Daniels, and M.R. Ehsani (eds.) Handbook of agricultural geophysics, CRC Press, Taylor & Francis, Boca Raton, FL, pp. 3–16.

Allred, B.J., D. Groom, M.R. Ehsani, and J.J. Daniels. 2008b. Resistivity methods. *In* B.J. Allred, J.J. Daniels, and M.R. Ehsani (eds.) Handbook of agricultural geophysics, CRC Press, Taylor & Francis, Boca Raton, FL, pp. 85–108.

Allred, B.J., R.S. Freeland, H.J. Farahani, and M.E. Collins. 2010. Agricultural geophysics: Past, present, and future. *In* Proceedings of the Symposium on the Application of Geophysics to Engineering and Environmental Problems (SAGEEP) 2010, pp. 190–202.

Arruda, N., and D.A. Grimley. 2002. Using magnetic susceptibility to delineate hydric soils in Illinois: Evidence for magnetic dissolution. Geological Society of America Joint Annual Meeting, Paper 45–0.

Bartington Instruments. 2016. Magnetic susceptibility equipment. http://www.bartington.com/magnetic-susceptibility-systems.html [Accessed 12 September 2016]

Beaudette, D.E., L.K. Stupi, A. Swarowsky, A.T. O'Green, J.F. Chang, and B. Gallagher. 2009. Watershed-scale geochemical inventory of soils by portable X-ray fluorescence. Eos, Transactions American Geophysical Union, 90(52), Fall Meeting Supplement, Abstract B11A0467B, San Francisco, CA.

Christy, C.D. 2008. Real-time measurement of soil attributes using on-the-go near infrared reflectance spectroscopy. Computers and Electronics in Agriculture 61(1):10–19.

Conyers, L.B. 2004. Ground-penetrating radar for archaeology. AltaMira Press, Walnut Creek, CA.

Corwin, D.L. 2008. Past, present, and future trends in soil electrical conductivity measurements using geophysical methods. *In* B.J. Allred, J.J. Daniels, and M.R. Ehsani (eds.) Handbook of agricultural geophysics, CRC Press, Taylor & Francis, Boca Raton, FL, pp. 17–44.

Dalan, R.A. 2006. Magnetic susceptibility. *In* J.K. Johnson (ed.) Remote sensing in archaeology: An explicitly North American perspective, Alabama Press, Tuscaloosa, AL, pp. 161–203.

Dalan, R.A., and S.K. Banerjee. 1996. Soil magnetism, an approach for examining archaeological landscapes. Geophysical Research Letters 23(2):185–188.

Daniels, D.J. 2004. Ground penetrating radar, 2nd edition. The Institute of Electrical Engineers, London, United Kingdom.

Daniels, R.B. 1987. Saline seeps in the Northern Great Plains of the USA and the Southern Prairies of Canada. *In* M.G. Wolman and F.G.A. Fournier (eds.) Land transformation in agriculture, John Wiley and Sons, pp. 381–406.

Dao, L., L. Morrison, and C. Zhang. 2012. Bonfires as a potential source of metal pollutants in urban soils, Galway, Ireland. Applied Geochemistry 27:930–935.

De Jong, E., D.J. Pennock, and P.A. Nestor. 2000. Magnetic susceptibility of soils in different slope positions in Saskatchewan, Canada. Catena 40:291–305.

Dearing, J.A., K.L. Hay, S.M.J. Baban, A.S. Huddleston, E.M.H. Wellington, and P.J. Loveland. 1996. Magnetic susceptibility of soil: An evaluation of conflicting theories using a national data set. Geophysical Journal International 127:728–734.

Doolittle, J.A., and E.C. Brevik. 2014. The use of electromagnetic induction techniques in soils studies. Geoderma 223-225:33–45.

Doolittle, J.A., and J.R. Butnor. 2008. Soils, peatlands, and biomonitoring. *In* H.M. Jol (ed.) Ground penetrating radar: Theory and applications (chapter 6), Elsevier, Amsterdam, The Netherlands, pp. 179–202.

Doolittle, J., J. Chibirka, E. Muniz, and R. Shaw. 2013. Using EMI and P-XRF to characterize the magnetic properties and the concentration of metals in soils formed over different lithologies. Soil Horizons 54(3):1–10. DOI: 10.2136/sh13-01-0009.

Ferrara, G., and J.A. Flore. 2003. An evaluation of the early-time GPR amplitude technique for electrical conductivity monitoring. Biologia Plantarum 46(1):41–47.

Fialová, H., G. Maier, E. Petrovský, A. Kapička, T. Boyko, and R. Scholger. 2006. Magnetic properties of soils from sites with different geological and environmental settings. Journal of Applied Geophysics 59:273–283.

Fine, P., M.J. Singer, R. La Ven, K. Verosub, and R.J. Hubbard. 1989. Role of pedogenesis in distribution of magnetic susceptibility in two California chronosequences. Geoderma 44:287–306.

Galagedara, L.W., G.W. Parkin, J.D. Redman, P. von Berktold, and A.L. Endres. 2005. Field studies of the GPR ground wave method for estimating soil water content during irrigation and drainage. Journal of Hydrology 301:182–197.

Gebbers, R., E. Lück, M. Dabas, and H. Domsch. 2009. Comparison of instruments for geoelectrical soil mapping at the field scale.

Near Surface Geophysics 7(3):179–190. DOI: 10.3997/1873-0604.2009011.

Geometrics, Inc. 2001. OhmMapper TR1 Operation manual. http://www.geometrics.com/geometrics-products/geometrics-electro-magnetic-products/electro-magnetic-information-and-case-studies/ [Accessed 12 September 2016]

Geometrics, Inc. 2016. G-858 MagMapper. http://www.geometrics.com/geometrics-products/geometrics-magnetometers/g-858-magmapper/ [Accessed 12 September 2016]

Greenhouse, J.P., and D.D. Slaine. 1983. The use of reconnaissance electromagnetic methods to map contaminant migration. Ground Water Monitoring Review 3(2):47–59.

Grimley, D.A., and M.J. Vepraskas. 2000. Magnetic susceptibility for use in delineating hydric soils. Soil Science Society of America Journal 64:2174–2180.

Grimley, D.A., N.K. Arruda, and M.W. Bramstedt. 2004. Using magnetic susceptibility to facilitate more rapid, reproducible and precise delineation of hydric soils in the Midwestern USA. Catena 58:183–213.

Grote, K., S. Hubbard, and Y. Rubin. 2003. Field-scale estimation of volumetric water content using GPR groundwave techniques. Water Resources Research 39(11):1321–1334.

Grote, K., T. Crist, and C. Nickel. 2010. Experimental estimation of the GPR groundwave sampling depth. Water Resources Research 46, Article W10520. DOI: 10.1029/2009WR008403.

Hanesch, M., and R. Scholger. 2005. The influence of soil type on magnetic susceptibility measured throughout soil profiles. Geophysical Journal International 161:50–56.

Hemmat, A., and V.I. Adamchuk. 2008. Sensor systems for measuring spatial variation in soil compaction. Computers and Electronics in Agriculture 63(2):89–103.

Huisman, J.A., S.S. Hubbard, J.D. Redman, and A.P. Annan. 2003. Monitoring soil water content with ground-penetrating radar: A review. Vadose Zone Journal 2:476–491.

Islam, K., B. Singh, and A. McBratney. 2003. Simultaneous estimation of several soil properties by ultra-violet, visible, and near-infrared reflectance spectroscopy. Australian Journal of Soil Research 41(6):1101–1114.

Jones, S.B., J.M. Wraith, and D. Or. 2002. Time domain reflectometry measurement principles and applications. Hydrological Processes 16:141–153.

Kalnicky, D.J., and R. Singhvi. 2001. Field portable XRF analysis of environmental samples. Journal of Hazardous Materials (83):93–122.

Lobred, A.R., and J.E. Simms. 2009. Application of magnetic susceptibility for wetland delineation. Proceedings of the Symposium on the Application of Geophysics to Engineering and Environmental Problems (SAGEEP) 22:559–570.

Loke, M.H. 2014. RES2DINV. Geotomo Software, Penang, Malaysia. http://www.geotomosoft.com [Accessed 6 September 2016]

Lu, Z., C.J. Hickey, and J.M. Sabatier. 2004. Effects of compaction on the acoustic velocity in soil. Soil Science Society of America Journal 68:7–16.

Lück, E., R. Gebbers, J. Ruehlmann, and U. Sprangenberg. 2009. Electrical conductivity mapping for precision farming. Near Surface Geophysics 7(1):15–25.

Lund, E.D., C.D. Christy, and P.E. Drummond. 2000. Using yield and soil electrical conductivity (EC_a) maps to derive crop production performance information. *In* P.C. Roberts, R.H. Rust, and W.E. Larson (eds.) Proceedings of the 5th International Conference on Precision Agriculture (CD-ROM), Minneapolis, Minnesota, 16–19 July 2000, American Society of Agronomy, Madison, WI.

Magiera, T., Z. Strzyszcz, A. Kapička, and E. Petrovský. 2006. Discrimination of lithogenic and anthropogenic influences on topsoil magnetic susceptibility in Central Europe. Geoderma 130:299–311.

Maier, G., R. Scholger, and J. Schön. 2006. The influence of soil moisture on magnetic susceptibility measurements. Journal of Applied Geophysics 59:162–175.

McNeill, J.D. 1980. Electromagnetic terrain conductivity measurement at low induction numbers. Technical Note TN–6. Geonics Limited, Mississauga, Ontario, Canada.

Mouazen, A.M., B. Kuang, J. De Baerdemaeker, and H. Ramon. 2010. Comparison among principal component, partial least squares and back propagation neural network analyses for accuracy of measurement of selected soil properties with visible and near infrared spectroscopy. Geoderma 158(1–2):23–31.

Mullins, C.E. 1977. Magnetic susceptibility of the soil and its significance in soil science: A review. Journal of Soil Science 28:223–246.

Oelze, M.L., W.D. O'Brien, Jr., and R.G. Darmody. 2002. Measurement of attenuation and speed of sound in soils. Soil Science Society of America Journal 66:788–796.

Olson, C.G., and J.A. Doolittle. 1985. Geophysical techniques for reconnaissance investigations of soils and surficial deposits in

mountainous terrain. Soil Science Society of America Journal 49(6):1490–1498.

Rogers, M.B., J.R. Cassidy, and M.I. Dragila. 2005. Ground-based magnetic surveys as a new technique to locate subsurface drainage pipes: A case study. Applied Engineering in Agriculture 21:421–426.

Roth, K., R. Schulin, H. Fluhler, and W. Attinger. 1990. Calibration of time domain reflectometry for water content using a composite dielectric approach. Water Resources Research 26(10):2267–2273.

Samouëlian, A., I. Cousin, A. Tabbagh, A. Bruand, and G. Richard. 2005. Electrical resistivity survey in soil science: A review. Soil & Tillage Research 83:173–193.

Schrader, C.D., and R.J. Stinner. 1961. Remote analysis of surfaces by neutron-gamma-ray inelastic scattering technique. Journal of Geophysical Research 66:1951–1956.

Schwarz, K., S.T.A. Pickett, R.G. Lathrop, K.C. Weathers, R.V. Pouyat, and M.L. Cadenasso. 2012. The effects of the urban built environment on the spatial distribution of lead in residential soils. Environmental Pollution 163:32–39.

Schwertmann, U., and R.M. Taylor. 1989. Iron oxides. *In* J.B. Dixon and S.B. Weed (eds.) Minerals in soil environments, Soil Science Society of America, Madison, WI, pp. 145–180.

Serbin, G., and D. Or. 2003. Near-surface soil water content measurements using horn antenna radar: Methodology and overview. Vadose Zone Journal 2:500–510.

Shamatava, I., B.E. Barrows, F. Shubitidze, B. Zhang, L. O'Neill, P. Fernández, and K.P. Paulsen. 2007. Estimating magnetic susceptibility from EMI data. *In* R.S. Harmon, J. Thomas Broach, and J.H. Holloway (eds.) Detection and remediation technologies for mines and minelike targets XII, Proceedings of SPIE, Vol. 6553. DOI: 10.1117/12.720034.

Smith, D.G., and H.M. Jol. 1995. Ground-penetrating radar: Antenna frequencies and maximum probable depths of penetration in Quaternary sediments. Journal of Applied Geophysics 33:93–100.

Soil Survey Staff. 2015. Web Soil Survey. USDA Natural Resources Conservation Service. http://websoilsurvey.nrcs.usda.gov/ [Accessed 1 August 2016]

Sudduth, K.A., N.R. Kitchen, W.J. Wiebold, W.D. Batchelor, G.A. Bollero, D.G. Bullock, D.E. Clay, H.L. Palm, F.J. Pierce, R.T. Schuler, and K.D. Thelen. 2005. Relating apparent electrical conductivity to soil properties across the north-central USA. Computers and Electronics in Agriculture 46:263–283.

Tabbagh, A. 1986. What is the best coil orientation in the Slingram electromagnetic prospecting method? Archaeometry 28:185–196.

Topp, G.C., J.L. Davis, and A.P. Annan. 1980. Electromagnetic determination of soil water content: Measurements in coaxial transmission lines. Water Resources Research 16:574–582.

Trimble Navigation Ltd. 2016. AgGPS 132 DGPS receiver/AgGPS 132 FlightBar system. http://www.trimble.com/agriculture/technical_support.aspx?id=4359 [Accessed 12 September 2016]

Vadyunina, A.F., and V.F. Babanin. 1972. Magnetic susceptibility of some soils in the USSR. Soviet Soil Science 4:588–599.

Vadyunina, A.F., and Y.A. Smirnov. 1978. Use of magnetic susceptibility in the study and mapping of soils. Pochvovedeniye, Moscow, Russia.

van Overmeeren, R., S. Sariowan, and J. Gehrels. 1997. Ground penetrating radar for determining volumetric soil water content; Results of comparative measurements at two test sites. Journal of Hydrology 197:316–338.

Veris Technologies. 2016. Soil EC 3100. http://www.veristech.com/the-sensors/v3100 [Accessed 12 September 2016]

Viscarra Rossel, R.A., M. Gilbertson, L. Thylén, O. Hansen, S. McVey, and A.B. McBratney. 2005. Field measurements of soil pH and lime requirement using an on-the-go soil pH and lime requirement measurement system. Precision Agriculture, European Conference on Precision Agriculture, pp. 511–520.

Viscarra Rossel, R.A., D.J.J. Walvoort, A.B. McBratney, L.J. Janik, and J.O. Skjemstad. 2006. Visible, near infrared, mid infrared or combined diffuse reflectance spectroscopy for simultaneous assessment of various soil properties. Geoderma 131(1–2):59–75.

Viscarra Rossel, R.A., H.J. Taylor, and A.B. McBratney. 2007. Multivariate calibration of hyperspectral γ-ray energy spectra for proximal soil sensing. European Journal of Soil Science 58:343–353.

Viscarra Rossel, R.A., S.R. Cattle, A. Ortega, and Y. Fouad. 2009. *In situ* measurements of soil colour, mineral composition and clay content by vis-NIR spectroscopy. Geoderma 150(3-4):253–266.

Viscarra Rossel, R.A., V.I. Adamchuk, K.A. Sudduth, N.J. McKenzie, and C. Lobsey. 2011. Proximal soil sensing: An effective approach for soil measurements in space and time, chapter 5. Advances in Agronomy 113:237–283.

Walker, J.P., and P.R. Houser. 2002. Evaluation of the OhmMapper instrument for soil moisture measurement. Soil Science Society of America Journal 66:728–734.

Wang, C.H., D.L. Willis, and W.D. Loveland. 1975. Radiotracer methodology in the biological environmental and physical sciences.

Prentice-Hall Biological Science Series, Prentice Hall, Englewood Cliffs, NJ.

Weindorf, D.C., Y. Zhu, R. Ferrell, N. Rolong, T. Barnett, B.L. Allen, J. Herrero, and W. Hudnall. 2009. Evaluation of portable X-ray fluorescence for gypsum quantification in soils. Soil Science 174(10):556–562.

Weindorf, D.C., Y. Zhu, B. Haggard, J. Lofton, S. Chakraborty, N. Bakr, W. Zhang, W.C. Weindorf, and M. Legoria. 2012a. Enhanced pedon horizonation using portable X-ray fluorescence spectrometry. Soil Science Society of America Journal 76(2):522–531.

Weindorf, D.C., Y. Zhu, S. Chakraborty, N. Bakr, W. Zhang, and B. Huang. 2012b. Enhanced use of portable X-ray fluorescence spectrometry for environmental quality assessment of peri-urban agriculture. Environmental Monitoring and Assessment 184:217–227.

Wielopolski, L., G. Hendrey, K.H. Johnsen, S. Mitra, S.A. Prior, H.H. Rogers, and H.A. Torbert. 2008. Nondestructive system for analyzing carbon in the soil. Soil Science Society of America Journal 72(5):1269–1277.

Zwanka, W.P., G.W. Hurt, D.A. Graetz, W.D. Graham, and M.W. Clark. 2007. Using magnetic susceptibility to delineate hydric soils in southeastern Coastal Plain soils. Soil Survey Horizons 48(2):32–38.